

# GUIDEWIRE TRACKING WITH PROJECTED THICKNESS ESTIMATION

Tomislav Petković and Sven Lončarić

University of Zagreb  
Faculty of Electrical Engineering and Computing  
Unska 3, Zagreb, Croatia

## ABSTRACT

Real-time guidewire tracking provides valuable navigational aid during endovascular procedures and is an important problem in computer-aided interventions. We propose an extension to the background estimation tracking method in order to enable estimation of the projected guidewire thickness. First, we use a combination of MAP estimation and Kalman filtering for background modeling. Second, the obtained background is used for guidewire tracking and for projected thickness estimation. The x-ray data acquisition model is used to estimate the thickness. The projected guidewire thickness provides insight into the 3D position of the object and can be used to improve monoplane 3D tracking. Estimated position of the guidewire compares favorably to the existing state of the art methods such as Hessian eigenvalue analysis.

*Index Terms*— x-ray fluoroscopy, guidewire tracking

## 1. INTRODUCTION

Endovascular interventional procedures are becoming more and more sophisticated thus requiring equipment capable of giving better support to the physician. X-ray fluoroscopy is preferred aid when navigating the guidewire through the tortuous vessels. A reliable and robust monoplane guidewire tracking with possible reconstruction of the actual 3D position would be a welcome improvement as it simplifies the procedure.

In this article we describe a fast method for 2D guidewire tracking during endovascular interventions. We assume the patient is motionless,<sup>1</sup> thus making application of the background modeling techniques possible. Similar approach that utilizes background modeling was described by Takemura et al. [1]. Another approach for guidewire detection is based on the eigenanalysis of the Hessian matrix as described by Baert et al. [2] and by Zarge et al. [3]. All of the aforementioned methods are primarily focused on guidewire detection and tracking, however, by using X-ray image formation model we can extract additional information from the 2D fluoroscopic

<sup>1</sup>The described technique is currently limited to applications where background is stationary, ie. neurosurgery. It cannot be used for tracking during procedures where pulsations are noticeable.

sequence such as projected thickness. Obtained information can then be utilized to improve monoplane guidewire reconstruction as described by Walsum et al. [4].

## 2. BACKGROUND MODEL

If an homogeneous and isotropic object is placed between X-ray source and detector the observed intensity can be approximated by  $I = \int I_0(E)e^{-\mu(E)s} dE$ , where  $I_0(E)$  is the source intensity,  $\mu(E)$  [cm<sup>-1</sup>] is the linear attenuation coefficient and  $d$  [cm] is the object thickness [5, 6]. Attenuation coefficient  $\mu$  depends on both the material and X-ray energy. However, for the narrow energy band a good approximation is  $I = I_0e^{-\mu d}$ , or by allowing for more than one material

$$I = I_0e^{-\sum_i \mu_i d_i}. \quad (1)$$

If we assume the patient is motionless (1) models the observed intensity. So the quantity  $-\sum_i \mu_i d_i$  summarizes the total attenuation. For guidewire to be visible a material having the large attenuation coefficient  $\mu_{\text{gw}}$  is used, so to make detection possible  $d_{\text{gw}}\mu_{\text{gw}} \gg \sum_i \mu_i d_i$  should hold. We also assume the guidewire is thin compared to the total tissue thickness, so  $d_{\text{gw}} \ll \sum_i d_i$  thus also making tissue compression unnoticeable.

For the case of the motionless patient if the guidewire is not on the actual X-ray path observed intensity is

$$I_1 = I_0e^{-\sum_i \mu_i d_i}. \quad (2)$$

During the procedure when the wire reaches some position instead of intensity (2) we expect to measure

$$I_2 = I_0e^{-d_{\text{gw}}\mu_{\text{gw}} - \sum_i \mu_i d_i}. \quad (3)$$

### 2.1. MAP Estimation of the Background

Measured intensities given by (2) and (3) do not account for the noise. There are several noise sources, but truly limiting for all practical purposes is the photon statistical noise [5], so we model the X-ray detector as a photon counting system with all other noise sources being disregarded.

Let us denote the intensities we should observe by  $b(x, y)$  and the actually observed ones by  $g(x, y)$ . The number of

photons contributing to  $g(x, y)$  can be described by Poisson random variable with mean  $b(x, y)$ . We assume all  $b(x, y)$  are independently generated with known mean  $\mu_b(x, y)$  and variance  $\sigma_b(x, y)$  for each position making the  $g(x, y)$  also independent. Conditional probability density of  $g(x, y)$  is Poissonian with mean  $b(x, y)$ . Under those assumptions MAP estimate of the ideal background  $b(x, y)$  for positions where the guidewire is absent is given by Rabbanai [7] as

$$b_{\text{MAP}}(x, y) = \frac{1}{2} \left( \mu_b(x, y) - \sigma_b^2(x, y) + \sqrt{(\mu_b(x, y) - \sigma_b^2(x, y))^2 + 4\sigma_b^2(x, y)g(x, y)} \right). \quad (4)$$

To track the background parameters we can use Kalman filtering [8] with the input being the MAP background estimate (4).

## 2.2. Kalman Filtering for Background Estimation

As mentioned in the section 2 we assume background values  $b(x, y)$  can be modeled by a Gaussians with known mean and variance. Each  $b(x, y)$  corresponds to one image pixel, with pixels being independently generated. This model makes Kalman filtering [8] a natural choice for tracking the changes of the background mean and variance. For a pixel at location  $(x, y)$  in the detector plane we can write the equations (coordinates are omitted for clarity)

$$\begin{aligned} b[n] &= b[n-1] + Q_1[n] \\ i[n] &= H[n]b[n] + Q_2[n] \end{aligned} \quad (5)$$

where  $b[n]$  is the background value for the current time step if the guidewire is not present,  $i[n]$  is the intensity we should observe and  $Q_1[n]$  and  $Q_2[n]$  are independent additive white Gaussian random processes.  $Q_1[n]$  should be chosen in a way to accommodate small variations in the background (i.e. extremely weak pulsations).  $H[n]$  is the *time dependent* measurement coefficient.

Background  $b[n]$  is time independent if the patient does not move. In the absence of the guidewire the value of background  $b[n]$  for each position  $(x, y)$  is given by (2). However, if the guidewire moves so we observe it in the position  $(x, y)$  we would expect to measure the value given by (3), and that is clearly not  $b[n]$  we expect. Term  $H[n]$  is used to model such variation. Image intensity  $i[n]$  we expect to measure is given either by (2) or (3). Disregarding the noise we have

$$i[n] = I_0 e^{-\sum_i \mu_i d_i} + Q_2[n] \quad (6)$$

if the guidewire is absent, and

$$i[n] = I_0 e^{-d_{\text{gw}} \mu_{\text{gw}} - \sum_i \mu_i d_i} + Q_2[n] \quad (7)$$

if the guidewire is present. Term  $H[n]$  is clearly time dependent. Comparison of (6) and (7) shows

$$H[n] = \begin{cases} 1, & \text{in the absence of the guidewire} \\ e^{-d_{\text{gw}} \mu_{\text{gw}}}, & \text{otherwise} \end{cases}. \quad (8)$$

Equations (5) and (8) define the time dependent linear dynamical system and Kalman filtering can be used to obtain the background state estimate  $b[n]$ . Prediction equations of the Kalman filter are

$$\begin{aligned} \hat{b}^-[n] &= \hat{b}[n-1] \\ P^-[n] &= P[n-1] + R_{Q_1 Q_1} \end{aligned} \quad (9)$$

while the new background estimate  $\hat{b}[n]$  is obtained as

$$\begin{aligned} K[n] &= P^-[n]H[n](H^2[n]P^-[n] + R_{Q_2 Q_2})^{-1} \\ &= \frac{P^-[n]H[n]}{H^2[n]P^-[n] + R_{Q_2 Q_2}} \\ \hat{b}[n] &= \hat{b}^-[n] + K[n](i[n] - H[n]\hat{b}^-[n]) \\ P[n] &= (1 - K[n]H[n])P^-[n] \end{aligned} \quad (10)$$

By computing (9) and (10) we obtain the optimal background estimate for each pixel. Guidewire positions and projected thickness are determined by the value of  $H[n]$ . It is important to note that  $H[n]$  is *time dependent* meaning we cannot, in advance, know what value  $H[n]$  takes for each step  $n$ , and that is precisely the information we want to obtain.

## 3. GUIDEWIRE TRACKING

The problem consists of detecting the moving guidewire under the stationary background assumption. To solve this we must derive a way of determining  $H[n]$  for every pixel. Normally, one would expect to use the simple background subtraction as the background is known, however the result of subtraction would be modulated by the image intensity.<sup>2</sup> Instead of subtracting the background we must compute the ratio between the background and the input image.

Disregarding the noise the measured intensity for each pixel is given by (2) or (3). The ratio of those intensities is  $I_1 : I_2 = \exp(d_{\text{gw}} \mu_{\text{gw}})$ . For each step  $n$  prior estimate  $\hat{b}^-[n]$  is the background we expect so the ratio  $\hat{b}^-[n] : i[n]$  is

$$\frac{\hat{b}^-[n]}{i[n]} \approx \frac{\hat{b}^-[n]}{H[n-1]\hat{b}^-[n] + Q_2[n]}, \quad (11)$$

where instead of  $H[n]$  we used  $H[n-1]$  (causality). If noting moves we expect  $H[n] = H[n-1]$  and the ratio (11) should be equal or near to 1 as  $\mathbb{E}[Q_2[n]] = 0$ .

If the ratio (11) differs from the expected value  $H[n]$  must be adjusted accordingly. If the ratio is significantly larger than

<sup>2</sup>It can be easily shown by computing  $i[n] - i[n-1]$  and using (6) and (7). Most visual tracking literature uses subtraction to detect movement meaning we should compute  $i[n] - H[n]\hat{b}^-[n]$  and compare the subtraction result to some threshold. Let  $H[n] = 1$  and let us disregard the noise. By (6) and (7) we have  $I_0 e^{-\sum_i \mu_i d_i} - I_0 e^{-d_{\text{gw}} \mu_{\text{gw}} - \sum_i \mu_i d_i} = (1 - e^{-d_{\text{gw}} \mu_{\text{gw}}}) I_0 e^{-\sum_i \mu_i d_i}$ . Value of  $I_0 \exp(-\sum_i \mu_i d_i)$  cannot be known in advance meaning fixed threshold cannot be used. Small value of this term makes detection difficult regardless of the  $e^{-d_{\text{gw}} \mu_{\text{gw}}}$ .

one we can assume the guidewire moved to that particular position in the time step  $n$ . On the other hand, if the ratio is significantly smaller than the guidewire moved away. Exact value of ratio threshold can be chosen by examining probability densities of the  $\frac{\hat{b}^-[n]}{i[n]}$  for two cases, absent and present guidewire, and selecting it to minimize the classification error. This reasoning now enables us to construct the rules used to change the value of  $H[n]$ :

1. For each new image we compute the  $b_{\text{MAP}}[n]$ . For the  $\mu_b$  and  $\sigma_b$  we use the prior estimates from Kalman filter ( $\mu_b = \hat{b}^-[n]$ ,  $\sigma_b^2 = P^-[n]$ ).
2. We compute the ratio between the  $\hat{b}^-[n]$  and  $b_{\text{MAP}}[n]$ . If the computed ratio is larger than the preset threshold (that is greater than one) we set  $H[n]$  to be of the form  $\exp(-d_{\text{gw}}\mu_{\text{gw}})$ . If the computed ratio is lower than the threshold we reset  $H[n]$  to be equal to one.
3. We proceed with Kalman filtering by computing (9) and (10).

If we allow only one guidewire thickness  $H[n]$  will switch between one and  $\exp(-d_c\mu_c)$ .

#### 4. PROJECTED THICKNESS ESTIMATION

The measurement coefficient  $H[n]$  does not only contain the information about the position of the guidewire, it also encodes projected guidewire thickness—not the wire radius, but the length of the path x-rays travel to pass through the wire. If the wire radius is  $r$  estimated thickness should always be greater,  $d_{\text{gw}}[n] \geq r$ . Estimated thickness can be a valuable clue, especially when used to facilitate reconstruction of 3D guidewire position from monoplane sequence.

Equation (8) limits possible values for  $H[n]$ . For image pixels where the guidewire is present

$$i[n] = H[n]b[n] + Q_2[n] = r^{-d_{\text{gw}}[n]\mu_{\text{gw}}}b[n] + Q_2[n] \quad (12)$$

holds. As we do not know the value of  $d_{\text{gw}}$  in advance equations (9) and (10) cannot be used without modification.

Let us assume the guidewire was detected for the time step  $k$  so ratio (11) was larger than the chosen threshold. Then  $\hat{b}^-[k]$  is the best background estimate. We cannot use the (9) and (10) directly, but putting  $\hat{b}^-[k]$  in (12) yields

$$i[n] = H[n]\hat{b}^-[k] + Q_2[n] \quad (13)$$

and together with

$$H[n] = H[n-1] + Q_3[n] \quad (14)$$

leads us to the new Kalman filter estimating the measurement coefficient  $H[n]$ . Here  $Q_3[n]$  is artificially added process noise that models expected change in  $H[n]$ . Starting variance of the  $H[n]$  can be computed from  $P^-[k]$  as  $\sigma_{H[k]}^2 =$

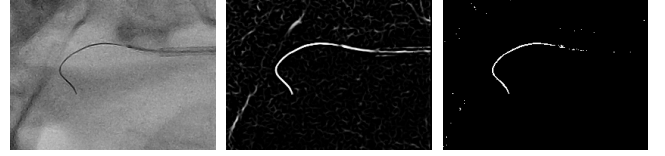


**Fig. 1.** A comparison of tracking results: the fluoroscopic image (left), the result of the analysis of the Hessian matrix eigenvalues (middle), and the result of the proposed tracking system (right).

**Table 1.** Contingency tables for the Hessian analysis and the proposed method

	Hessian analysis			Proposed method		
	Actual value		Total	Actual value		Total
	P	N		P	N	
P	12975	5878	18853	8753	10100	18853
N	4488	149255	153743	2694	151049	153743
Total	17463	155133	172596	11447	161149	172596

$\frac{i[k]}{\hat{b}^{-2}[k]}P^-[k]$ . The relation between measurement coefficient  $H[n]$  and the guidewire thickness  $d_{\text{gw}}[n]$  is logarithmic so we have  $d_{\text{gw}}[n] = -\frac{1}{\mu_{\text{gw}}}\log H[n]$ . As the term  $\mu_{\text{gw}}$  is usually not precisely known absolute thickness measurement is not possible without proper calibration, but relative thickness measurement is possible.

#### 5. RESULTS AND DISCUSSION

Described method was applied to one fluoroscopic image sequence consisting of 560 images yielding satisfactory results. When compared to the analysis of the eigenvalues of the Hessian matrix the proposed tracking method is lacking as it is unable to detect the stationary part (see Fig. as 1, proximal part), but it can yield additional information such as thickness.

As both the Hessian analysis and the proposed method are pixel classifiers the comparison of was done by comparing results with the manual segmentation for each frame. Manual segmentation was done for each frame as shown in fig. 2. The characteristic of both detectors is summarized in table 1 and figure 3.

The proposed thickness estimation is able to produce useful results, however as the calibration data for the sequence was not available only relative measurements were possible. Figure 4 shows the method can detect the increase in the thickness when the guidewire overlaps itself—measured average change in intensity is about 2, but the values are not stable due to noise ranging from 1.6 to 3.2 for the overlapped part. As only one x-ray sequence was available proposed method must be tested on larger number of datasets to determine the usefulness, especially as the aid to the 3D reconstruction.

Improvements are possible by introducing spatial rela-

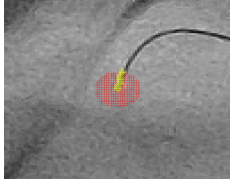


**Fig. 2.** A circular area around the tip showing manual segmentation. The area is centered around the tip and is made small as the primary application would be the wire tip detection.

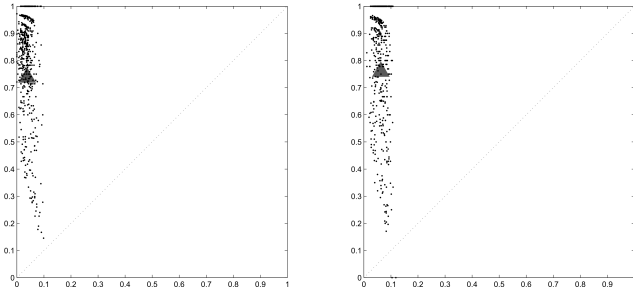


**Fig. 3.** TP vs. FP points for Hessian analysis (left) and the proposed method (right) for each frame in the sequence. Black points denote the characteristic for each individual frame, while the triangle denotes overall characteristic of both detectors.

tions into the computation of the MAP estimate and the background model, or by extending the model to encompass pulsating backgrounds. However, such extensions increase computational complexity significantly. By utilizing only temporal filtering to estimate the background spatial averaging of neighboring pixels is avoided thus preserving the fine anatomical details. Described guidewire detection algorithm can be easily implemented in real time. An experimental implementation using the Intel IPP operating on  $1024 \times 1024$  input images with 16 bits per pixel needs at most 40 ms on an average PC to process one frame.

## 6. CONCLUSION

We described the system to track and estimate guidewire position and thickness. Presented guidewire tracking reliably detects the moving guidewire. To improve detection results presented technique should be supplemented by combining it with other segmentation methods that are able to detect stationary wires. It should prove to be particularly useful tool not simply for guidewire tracking, but for combined tracking and 3D position reconstruction of guide wires or needles by using monoplane X-ray imaging devices only. Proposed tracking system is not computationally heavy and can achieve real time performance.

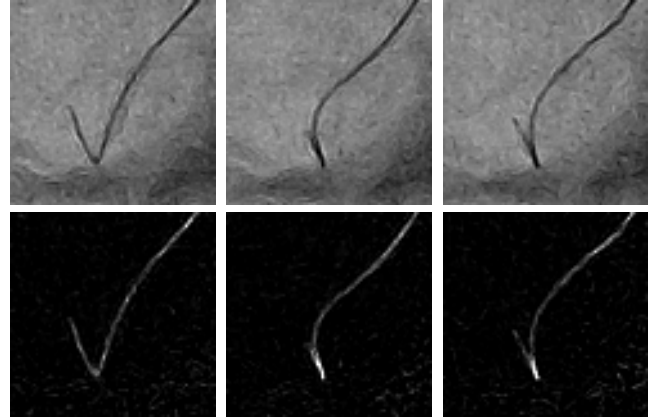


**Fig. 4.** Result of thickness estimation. Top row shows selected images from the input fluoroscopic sequence. Bottom row shows the estimated thickness. Note the intensity doubling where the guidewire overlaps itself.

## 7. REFERENCES

- [1] A. Takemura, K. R. Hoffmann, M. Suzuki, Z. Wang, H. S. Rangwala, H. Harauchi, S. Rudin, and T. Umeda, "An algorithm for tracking microcatheters in fluoroscopy," *Journal of Digital Imaging*, Feb. 2007.
- [2] S.A.M. Baert, M.A. Viergever, and W.J. Niessen, "Guidewire tracking during endovascular interventions," *IEEE Trans. Med. Imag.*, vol. 22, no. 8, pp. 965–972, Aug. 2003.
- [3] J. A. Zarge and N. R. Corby, "Method and apparatus for real-time tracking of catheter guide wires in fluoroscopic images during interventional radiological procedures," U.S. Patent 5,289,373, Feb. 1994.
- [4] T. van Walsum, S.A.M. Baert, and W.J. Niessen, "Guide wire reconstruction and visualization in 3dra using monoplane fluoroscopic imaging," *IEEE Trans. Med. Imag.*, vol. 24, no. 5, pp. 612–623, May 2005.
- [5] Bruce Hasegawa, *Physics of Medical X-Ray Imaging*, Medical Physics Publishing Corporation, revision of 2<sup>nd</sup> edition edition, 1987.
- [6] R. P. C. Schram, "X-ray attenuation—applicadon of X-ray imaging for density analysis," Tech. Rep. 20002/01.44395/I, NRG, Nov. 2001.
- [7] M. Rabbani, "Bayesian filtering of poisson noise using local statistics," *IEEE Trans. Acoust., Speech, Signal Process.*, vol. 36, no. 6, pp. 933–937, Jun 1988.
- [8] R. E. Kalman, "A new approach to linear filtering and prediction problems," *Transactions of the ASME—Journal of Basic Engineering*, vol. 82, no. Series D, pp. 35–45, 1960.